SIMULACIO MONTE CARLO DE SISTEMES AMB ACOBLAMENT DE GRAUS DE LLIBERTAT.

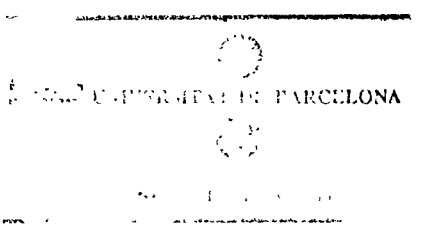

a) The change in slopes of E(T), see Fig. 3.

b) We have studied a number of local order parameters. Fig. 6a, shows the temperature dependence of the average $<|\psi|^2>$ and $|<\psi>|^2$ of the local orientational nearest neighbor parameter defined on each occupied cell as

$$\psi(r_i) = \frac{1}{6} \sum_{p=1}^{n_i} e^{i6\theta_{ip}}, \tag{8}$$

where the sum over p runs over the number of interacting neighbors n_i at site i, and θ_{ip} is the bond angle with respect to a reference axis. These parameters again shows clear anomalies (upon heating) at $T \sim 2$ for $U = 0$. On Fig. 6b is shown the positional particle fluctuation parameter $<u^2> = <r^2> - <r>^2$ around the ordered structure position - i.e. the reference lattice site. The parameter $<u^2>$ has an anomaly at the low temperature side of the transition region, again consistent with the anomaly in E(T) at $T \sim 1.55$ for $U = 0$. At higher temperatures it goes to the value 5/36, which is the theoretical value calculated assuming a random distribution of the particles inside the hexagonal cells. We have also considered an other, extrapolated definition of the positional fluctuations $<u^2>_e$ by fitting the distribution of particles inside the cells to a gaussian distribution of the form:

$$Ae^{-r^2/<u^2>_e}. \tag{9}$$

We have found that $<u^2>_e$ diverges at $T \sim 1.55$ for $U=0$. This is physically reasonable, and we preferentially use this definition in the following analyses.

c) We also followed the long range decrease of g(r) and that of the orientational order parameter $g_6(r)$ defined as

$$g_6(r) = \langle \psi(o)\, \psi^*(r) \rangle \qquad (10)$$

The available large r behavior was not found to be exponential, but is better described as an algebraic decay of the form

$$g(r) - 1 \sim r^{-\eta}, \quad g_6(r)/g(r) \sim r^{-\eta_6} \qquad (11)$$

This is demonstrated in Fig. 7b together with the temperature dependence of the exponents Fig. 7a. Possibly, we are not able to measure the decay at sufficiently large r to obtain an exponential decay, as expected from theory[4]. Here we are primarily using the variation of the long range behavior of the correlation functions as an indicator for the melting transition. We have found that both exponents show a clear anomaly at $T=2$ for $U = 0$ consistently with the change in E(T).

The phase diagram obtained in this way is shown in Fig. 8. Scans performed by varying T or U are indicated with heavy lines, the dots indicate that the lower phase boundary is rather more difficult to define accurately. As expected the transition temperature rises at first liniarily with increasing corrugation potential. This study is the first of the melting transition at coverage $c = 1/3$. It is in qualitative agreement with that of Barker et al.[29] for variable coverage $c < 1/3$.

V. Scattering properties

The main purpose of this paper is to discuss the behavior of the static structure factor $S(q)$, which can be measured in a X-ray or neutron scattering experiment. The structure factor is calculated as discussed in the Appendix A and defined as

$$S(q) \equiv \frac{1}{N_p^2} < \left| \sum_{i=1}^{N_p} e^{iq \cdot r_i} \right|^2 > . \qquad (12)$$

Where $N_p = N/3$ is the number of particles. It is normalized to 1 for $q = 0$ and approaches $1/N_p$ for $q \to \infty$. In the liquid phase the structure factor can be well fitted by a sum of Lorentzians and a slightly sloping, flat background as can be seen in Fig. 9. However, some small discrepancies are systematically present. Fig. 10a shows the evolution of $S(q)$ as a function of temperature for $U=0$. We follow three q - vectors, see Fig. 1b. The column indexed by q(11) shows the results for the q vector which contains the Bragg peaks at $q = (1,1)q_o/3$ and $(1,1)2q_o/3$ of the (chosen) ordered $\sqrt{3}\times\sqrt{3}$ structure of the reference lattice, $q_o = 4\pi/(\sqrt{3}a)$ is the wave vector unit, see Fig. 1. The q(21) column shows a low symmetry direction and the q(10) column the direction which contains the Bragg peak at $q=(1,0)q_o$ of a possible substrate together with a $\sqrt{3}\times\sqrt{3}$ Brag peak from the surface layer with the reference lattice structure. The q(11) sequence shows clearly the transformation of the large low temperature Bragg peaks. They have no width at $T=0$, but have developed "feet" at $T=0.5$. At the upper transition temperature $T=2$ these "feet" become the liquid diffuse scattering $S^{\ell}(q)$. The structure in the q(21) $S(q)$ at low T is due to the influence of the "feet" from the neighboring Bragg points. This is evident from Fig. 1. It is not a signature of liquid ring structure in the solid phase. At high temperature $T = 4$ the diffuse scattering forms an isotropic ring as demonstrated by the three cuts q(11), q(21) and q(10). Close to the melting point there is indication of some modulation of the ring (different from that expected for the initial lattice orientation). This feature needs further study. It probably disappears if an average is taken over many different runs.

Fig. 10b shows that a very similar behavior, at first sight, is obtained by varying the corrugation potential. An important difference is that the modulation of the ring in the liquid phase, for $U < 4.5$, shows a clear memory of the orientation of

the underlaying lattice. This is as expected. Another very important feature is the persistence of the Bragg peak at $q = (1,0)q_0$. This is the strongest sign of a lattice modulated liquid. In our simulation we, of course, do not see the substrate Bragg peak, but only the contribution from the surface layer. At the studied potential values no clear sign of peaks from possible secondary liquid rings around the (10) Bragg peaks are visible. A third important feature evident from the series of $S(q)$ on Fig. 10 is that there is no shift in the peak position of the first peak near the melting point. An accurate peak position was determined by Lorentzian fits as shown in Fig. 9. It must be remembered that we are studying the case of constant coverage and therefore a variable pressure. At constant pressure the position of the first peak may well move to smaller q-values in the liquid phase. It is therefore quite difficult to interpret a possible experimentally observed shift of the peak position, in particular as a sign of a hexatic phase. The induced contribution to the substrate Bragg peak $S(q_{10})$ has a number of interesting features. The peak intensity of $S(q_{10})$ is shown on Fig. 11a as a function of temperature for $U = 1$ and on Fig. 11b as a function of decreasing corrugation potential. It shows a clear anomaly in the transition region (close to the low T side) and in the liquid phase. The logarithm of the intensity decreases linearly towards the diffuse scattering of the liquid $S(q_{10}) \rightarrow 1/N_p = 0.00037$ for high T. The behavior as a function of decreasing corrugation potential Fig. 11b is qualitatively similar. In the Reiter and Moss linear theory[21] the intensity of the induced Bragg peak is solely dependent on the ratio (U/T), squared. The thin lines Fig. 11a and 11b are calculated using the first Fourier component Eq.(4). Since the expansion parameter for the theory is then approximately only - 1/10 of (U/T), the linear theory could be expected to apply to all our studied values of U and T in the liquid region. The fit is excellent for relatively large U and T, Fig. 11b. However, for small U the Bragg peak intensity obtained in the MC simulation starts larger, but falls off faster, Fig. 11a. In this case the corrugation potential is smaller than the energy corresponding to the melting temperature T_M. Notice the theory is

independent of T_M, directly. It is physically resonable that the Bragg peak is absorbed into the diffuse liquid structure factor for temperatures large relative to U and T_M. For small U the mean square positional fluctuation around the lattice sites for the corrugation potential $<r^2>/a^2$ is much larger close to T_M. We use the definition given in Eq. (9), $<r^2> = <u^2>_e + <r>^2$. On Fig. 12. is shown the temperature variation of $<r^2>/a^2$ for our potential for various U.

An interesting feature is that the Debye-Waller factor plot Fig. 13. shows that the peak intensity $S(q_{10})$ is an universal function of the mean square fluctuation $<r^2>/a^2$. Fig. 13. shows the same behavior irrespective of the relative values of U and T. This fact is very valuable and can be used to estimate the corrugation potential, when it is possible to calculate $<r^2>/a^2$. An experimental determination of $S(q_{10})$ as a function of T in combination with a plot like Fig. 12. allows a determination of U. The arrow at L indicates the Lindemann criterion[1] for melting in our case. The transition region in Fig. 8. falls in the range $L \leq <r^2>/a^2 \leq 0.3$.

VI Conclusion

The problem of two dimensional solids, liquids and melting has previously been investigated in the limits of either strong or weak interaction with a supporting substrate and for various coverage. In this paper we have instead studied a plane in phase space spanned by temperature T and a large interval of corrugation potentials U, mainly restricting the coverage to being fixed at 1/3, corresponding to a perfect $\sqrt{3}\times\sqrt{3}$ structure. The melting transition is found to occur in a monotonically increasing, relatively broad strip in the plane. The phase inside the strip, the transition region, has not been analyzed in detail in this paper. Under the constant coverage condition used, the pressure is rapidly increasing in the

transition region. This would lead to a mixed phase region at a discotiuous transition. Further studies are needed to establish the possible presence of a hexatic phase, but the different behavior of positional and orientational order parameters is not inconsistent with such a phase. The main emphasis has been laid on a investigation of the behavior of the experimentally observable structure factor. It is found that the position of the first peak does not change from that of the Bragg peak position neither in the transition region nor in the liquid. If such a shift is observed it is therefore a consequence of a pressure-density variation, which of course may be indirectly coupled to the melting and the transition region. The lineshape of the structure factor does not change noticably from the transition region to well into the liquid phase. The effect of a finite corrugation potential is most clearly seen in the persistence of a Bragg peak at $q = (1.0)q_0$ even in the liquid phase. This is due to the increased probability for (randomly) occupying the imaginary substrate lattice sites. As already emphasized by Reiter and Moss [21] this induced Bragg peak offers important possibilities for measuring the substrate potential U from the scattering data. We have here studied a large region of U and T. The theory[21] is a perturbation expansion in the ratio (U/T), The linear approximation predicts a Bragg peak intensity proportional to $(U/T)^2$. This theory fits the data excellently at relatively large U, close to the melting temperature, T_M. For small U the fit is less satisfactory. This seems at first sight surprising. The reason is that for small U the positional fluctuations $<r^2>$ around the lattice sites increase rapidly above T_M. This strongly influences the determination of a Bragg peak and its peak intensity. We have found that the logarithm of the intensity decreases linearly with increasing temperature beyond the transition region. We have further found that this intensity is an universal function, for various U and T, of the mean square displacement $<r^2>$ from the lattice sites. In the solid the exact Debye-Waller factor is found. In the modulated liquid another characteristic smaller factor is found. We have determined the temperature dependence of $<r^2>$ for some values of U and found a near linear increasing

behavior in the liquid phase. Since $<r^2>$ is strongly dependent on U and T and is easily calculable also for other models, a valuable tool to determine U has been found.

REFERENCES

1. K.J. Strandburg, Rev. Mod. Physics 60 (1988), 161

2. N.D. Mermin, Phys. Rev. 176 (1968), 250

3. J.M. Kosterlitz and D.J. Thouless, J. Phys. C: Solid State Phys. 6 (1973), 1181

4. B.I. Halperin and D.R. Nelson, Phys. Rev. Lett. 41 (1978), 121

5. P.A. Heiney, P.W. Stephens, R.J. Birgeneau, P.M. Horn and D.E. Moncton. Phys. Rev. B 28 (1983) 6416.

6. E.D, Specht, M. Sutton, R.J. Birgeneau, D.E. Moncton and P.M. Horn, Phys. Rev.B 30 (1984), 1589

7. D.E. Moncton, R. Pindak, S.C. Davey, G.S. Brown, Phys. Rev. Lett. 49 (1982) 1865.

8. F.F. Abraham, Phys. Rev. Lett. 44 (1980) 463

9. D. Frenkel and J.P. Mc Tague, Phys. Rev. Lett. 42 (1979), 1632

10. D.S. Fisher, B.I,. Halperin, R. Mart, Phys. Rev. B (1979) 20, 4692.

11. R. Birgeneau, P.M. Horn. Science 232 (1986), 329.

12. M.S. Dresselhaus and G. Dresselhaus, Adv. in Phys.30 (1981), 139

13. D.A. Huse, M.E. Fisher, Phys. Rev. B 29 (1984), 239.

14. A.G. Naumovets, Contemperary Physics 30 (1989), 187

15. S.W. Koch, F.F. Abraham. Phys. Rev. B 27 (1983) 2964

16. F.F. Abraham, Phys. Rev. Lett. 50 (1983), 978

17. D.P. Di Vicenzo, E.J. Mele Phys. Rev.B 32 (1985), 2538

18. A.N. Berker, S. Ostlund and F.A. Putham. Phys. Rev. B 17 (1978), 3650

19. R.G. Catlisch, A.N. Berker and M. Kardar Phys.Rev. B 31 (1985) 4527

20. N.C. Bartelt, T.L. Einstein, L.D. Roelofs. Phys. Rev. B 35 (1987), 1776

21. G. Reiter and C. Moss, Phys. Rev. B 33 (1986), 7209

22. F. Rousseaux, R. Moret, D. Guerard, P. Lagrange, M. Lelaurian. J. Phys (Paris) Lett 45 (1984) L111.

23. S.C. Moss, G. Reiter, J.L. Robertson, C. Thompson, and J.D. Fan, Phys. Rev.Lett. 57, (1986), 3191.

24. X.B. Kan, J.L. Robertson, S.C. Moss, K. Ohshima and C.J. Sparks, Phys. Rev. B39 (1989), 10627.

25. J.D. Fan, O.A. Karim, G. Reiter and S.C. Moss, Phys. Rev. B 39 (1989), 6111

26. E. Vives and A. Planes. Phys. Rev. A 41 (1990), 1885

27. F.F. Abraham in "Ordering in two dimensions" ed by S.K. Sinha, Elsevier, Holland (1980)

28. O.G. Mouritsen, "Computer studies of Phase Transitions and Critical Phenomena", Springer Verlag, Berlin (1989).

29. J.A. Barker, D. Henderson and F.F. Abraham, Physica 106A (1981) 226

Appendix A. Calculation of the structure factor

We can consider a system with *Periodic Boundary conditions* as a set of N' (N' ∞) replicas of our original LxL lattice ordered on a big superlattice with lattice spacing La. This "supercell" method was used by Fan et al[23], after a suggestion by A. Wrigth, for a calculation of the anisotropic structure factor. Subsequently an interpolation between the available points were made. Let us discuss a few details of the method. The structure factor for such system can be calculated as

$$S(q) = \frac{1}{N'^2 N_p^2} < \left| \sum_{K=1}^{N'} \sum_{i=1}^{N_p} e^{iq\cdot(X_K + x_i)} \right|^2 >$$

where the first sum is a sum over the different replicas of the system, the second sum is a sum over the N_p particles on the LxL lattice, X_K is a vector pointing to the origin of the different replicas and x_i is the position of the N_p particles inside the small lattice L×L (the unit cell.)Because the superlattice structure is independent of the thermal fluctuations we can split the sum into two factors:

$$S(q) = \frac{1}{N'^2} \left| \sum_{K=1}^{N'} e^{iq\cdot X_K} \right|^2 \frac{1}{Np^2} < \left| \sum_{i=1}^{N_p} e^{iq\cdot x_i} \right|^2 >$$

The first term gives a set of Bragg peaks corresponding to the superlattice structure, while the second one is the structure factor of a *finite* LxL system. As a consequence the $S(q)$ of our system will be only different from zero on a reciprocal lattice corresponding to a triangular lattice with spacing La, and hence the resolution in the reciprocal space will depend on the direction of q. In Fig. 1 we indicate the 3 directions that have been studied.

Because we have been working with L=90, we can only measure 90 points along the three different segments (0,0)-(1,0), (0,0)-(2,1), and (0,0)-(1,1). This means that the resolution is higher along the (1,0) direction than along the (1,1) direction and the (2,1) direction in particular. Statistical fluctuations can be reduced by averaging over several systems of size L×L. However, in order to increase the resolution it is necessary to increase the system size L. In fact one of the main reasons for using the Monte Carlo simulation, rather than molecular dynamics as in ref. 26, is that much lager L can be studied within reasonable computertime. We have not used interpolation between points in the structure factor.

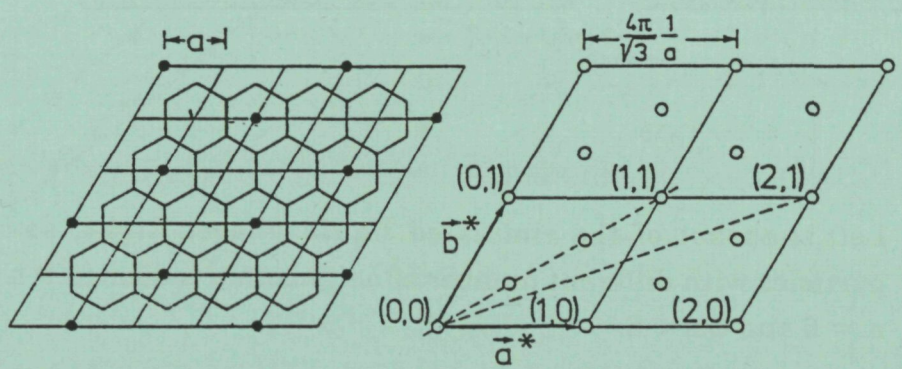

Fig. 1. Left, the direct reference lattice with the $\sqrt{3}\times\sqrt{3}$ structure indicated and the hexagonal cells. Right, the reciprocal space with the $\sqrt{3}\times\sqrt{3}$ Bragg peak positions indicated.

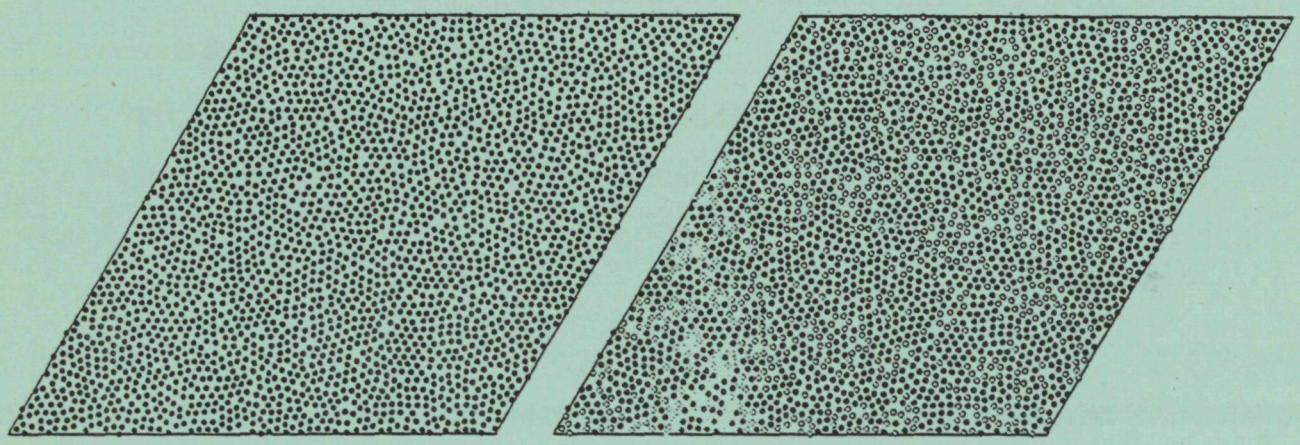

Fig. 2. Left,snapshot of the simulated liquid phase. Right, same with particles with different number of neighbors n indicated ● $n > 6$, ⊗ $n = 6$ and ○ $n < 6$.

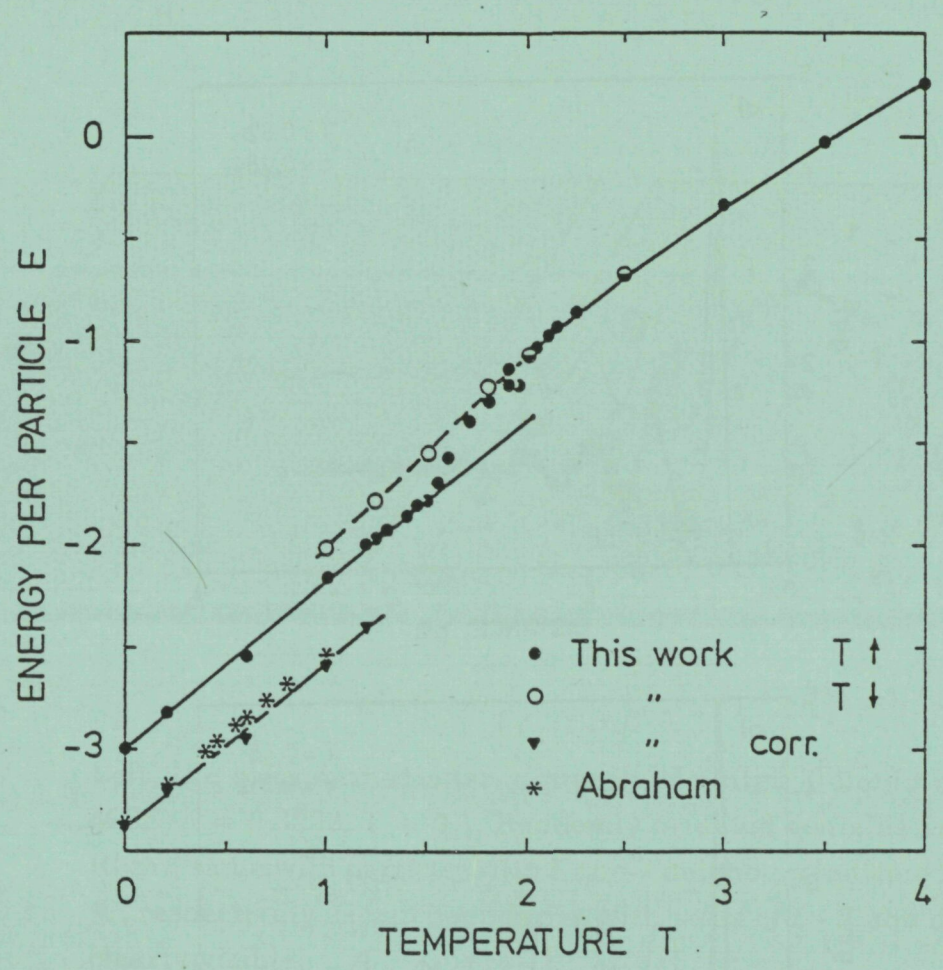

Fig. 3. The energy per particle as a function of temperature. The energy corrected for the effects of the cut-off $<\Delta H>_0$ agrees well with that obtained by Abraham[8].